AJNR

Reduced caliber of the internal carotid artery: a normal finding with ipsilateral absence or hypoplasia of the A1 segment.

A G Kane, W P Dillon, A J Barkovich, D Norman, C F Dowd and T T Kane

AJNR Am J Neuroradiol 1996, 17 (7) 1295-1301
http://www.ajnr.org/content/17/7/1295

Reduced Caliber of the Internal Carotid Artery: A Normal Finding with Ipsilateral Absence or Hypoplasia of the A1 Segment

Arthur G. Kane, William P. Dillon, A. James Barkovich, David Norman, Christopher F. Dowd, and Thomas T. Kane

PURPOSE: To determine whether a relationship exists between normal variations in anatomy of the circle of Willis and the size of the internal carotid arteries (ICA). **METHODS:** MR angiograms and axial MR images of the brains of 104 patients were reviewed. Included were 10 patients with unilateral absence of the A1 segment of the anterior cerebral artery, 10 with hypoplasia of one A1 segment, 28 with asymmetric A1 segments, nine with isolated unilateral fetal origin of the posterior cerebral artery, and 47 with balanced circulation. **RESULTS:** The mean ICA diameter measurement for the total population was 4.62 ± 0.68 mm. In patients with absent A1, the mean ipsilateral and contralateral ICA diameters were 3.63 ± 0.41 mm and 5.25 ± 0.52 mm, respectively. The mean percentages of the difference between the diameters of the right and left ICA (31% in the group with absent A1 and 21% in the group with hypoplastic A1) varied significantly from the differences in the ICA diameters among the rest of the population. The diameter differences produced by other common variations (unilateral small A1 segment or fetal origin of the posterior cerebral artery) did not differ significantly from those of the 47 patients with balanced intracranial circulation. **CONCLUSIONS:** There is an association of unilaterally absent or hypoplastic A1 segments of the anterior cerebral artery with ipsilateral decrease in ICA caliber, and this can be seen on MR angiograms.

Index terms: Arteries, anatomy; Arteries, carotid, internal; Magnetic resonance angiography

AJNR Am J Neuroradiol 17:1295–1301, August 1996

Unilateral reduction in the caliber of the intracavernous carotid artery seen on screening magnetic resonance (MR) images often suggests the possibility of either intracavernous carotid disease or more proximal bifurcation disease. The circle of Willis, which can be seen on MR angiograms, is not visible by means of conventional angiography owing to single-vessel injection. MR imaging and MR angiography provide accurate and direct comparisons of both the internal carotid and vertebrobasilar components of the intracranial circulation, as well as of the collateral circulation between them. We sought to establish which of the normal variations in intracranial circulation might result in asymmetry of the cavernous carotid arteries.

Materials and Methods

We reviewed 104 intracranial MR angiograms and corresponding MR images of the brain obtained between January 1993 and July 1995. The patients, 54 female and 50 male, were 3 through 84 years old (mean age, 54 ± 16 years). Patients with arteriovenous malformation or intracranial hemorrhage were excluded from the study.

All MR studies were done with a 1.5-T system. Three-dimensional time-of-flight MR angiograms were acquired from the level of the horizontal portion of the petrous segment of the internal carotid artery (ICA) to the genu of the corpus callosum. All MR angiography was done by using a 256 × 192 or 512 × 192 matrix with 0.9-mm-thick partition images. Multiplanar reformations in the oblique sagittal plane were performed through the cavernous segment of the ICA. Axial spin-echo images of the brain were

Received October 21, 1994; accepted after revision January 17, 1996.

Presented at the annual meeting of the American Society of Neuroradiology, Chicago, Ill, April 1995.

The opinions or assertions contained herein are the private views of the authors and are not to be construed as reflecting the views of the Department of the Army or the Department of Defense.

From the Department of Radiology, University of California, San Francisco (A.G.K., W.P.D., A.J.B., D.N., C.F.D.); A.M.E.D.D. Center and School, Fort Sam Houston, Tex (A.G.K.); and the School of Hygiene and Public Health, Johns Hopkins University, Baltimore, Md (T.T.K.).

Address reprint requests to Arthur G. Kane, MD, Department of Radiology, University of California, Neuroradiology Section, Box 0628, L-358, San Francisco, CA 94143.

AJNR 17:1295–1301, Aug 1996 0195-6108/96/1707–1295

Variations in the circle of Willis and in the caliber of the internal carotid artery

Normal Variant Category*	Mean, SD, Range of Right Carotid Diameter, mm	Mean, SD, Range of Left Carotid Diameter, mm	Sample Size, Mean Percentage (Range) of the Difference between Vessel Diameters
1. Absent A1			n=10, 31.1 (27–40)
R (n = 4)	3.60, 0.38, 3.0–4.0	5.25, 0.50, 4.5–6.0	
L (n = 6, 1L + 2BFP)	5.25, 0.58, 3.5–6.0	3.67, 0.44, 2.5–4.0	
2. Hypoplastic A1			n = 10, 21.0 (10–27)
R (n = 5)	4.30, 0.56, 3.5–5.5	5.30, 0.68, 4.5–7.0	
L (n = 5, 1L + 1RFP)	5.60, 0.52, 5.0–6.5	4.40, 0.48, 4.0–5.0	
3. Asymmetric A1			n = 28, 7.1 (0–20)
Small R (n = 14, 1L + 3RFP)	4.50, 0.64, 3.5–6.0	4.88, 0.66, 3.5–7.5	
Small L (n = 14, 3R + 1BFP)	5.15, 0.59, 3.5–6.5	4.89, 0.61, 4.0–6.0	
4. Isolated FP			n = 9, 6.9 (0–20)
R FP (n = 8)	4.75, 0.38, 4.0–5.0	4.50, 0.50, 3.5–5.5	
L FP (n = 1)	4.0, ..., ...	4.0, ..., ...	
5. Balanced circulation			n = 47, 3.1 (0–22)
Equal A1 (n = 43)	4.43, 0.52, 3.0–6.0	4.38, 0.52, 3.0–6.0	
Equal A1 with BFP (n = 4)	5.63, 1.13, 4.0–7.5	5.50, 1.25, 4.0–7.5	
Total (n = 104)	**4.65, 0.70, 3.0–7.5**	**4.59, 0.66, 2.5–7.5**	

Note.—B indicates bilateral; FP, fetal origin of posterior cerebral artery.

* *P* value by category: 1 (absent A1), $P < .00001$; 2, $P < .0001$; 3, $P > .14$; 4, $P > .24$.

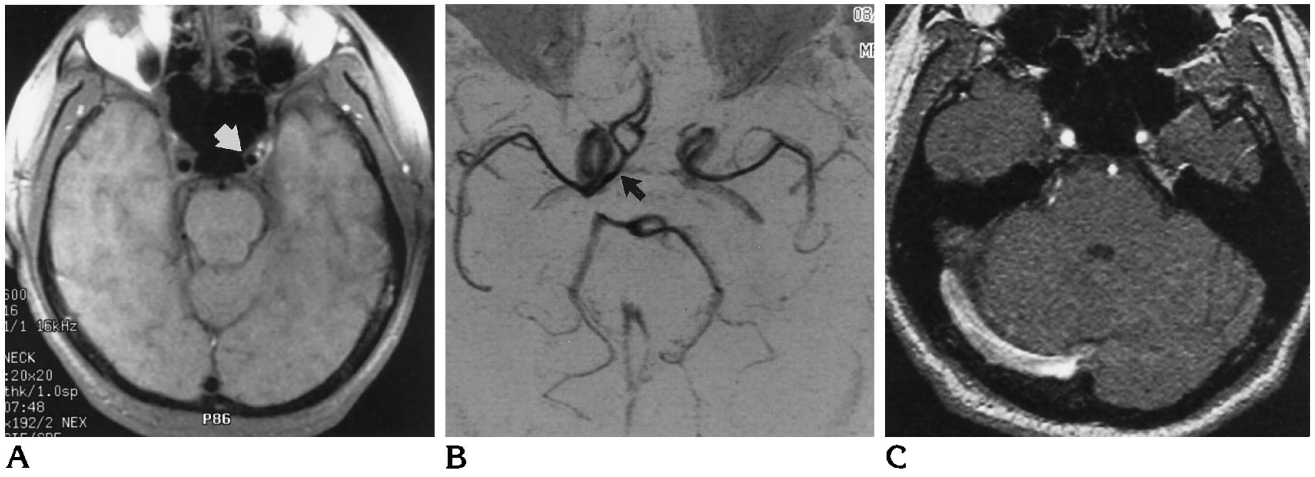

Fig 1. Absent left A1 segment of the ACA in a 28-year-old man with generalized headache.

A, Axial T1-weighted spin-echo MR image with fat saturation shows markedly reduced caliber of left ICA (*arrow*).

B, Collapsed view of 3-D time-of-flight MR angiogram shows absence of left A1 segment and reduced caliber of left ICA. The right A1 segment (*arrow*) gives rise to both anterior cerebral arteries. Findings on MR angiogram of the neck (not shown) were normal.

C, MR angiographic partition image at level of cavernous carotid artery shows asymmetry of vessel caliber.

obtained with inferior saturation pulses to minimize effects of the in-flow phenomenon.

Two neuroradiologists separately analyzed the images as follows. Maximum intensity projection and partition images were assessed for normal variations in the circle of Willis and grouped into five categories (see Table), which included four variations expected to produce differing sizes of the right and left ICA and a fifth category expected to produce equal sizes of the two sides. In the first variation, the A1 segment of the anterior cerebral artery (ACA) was considered to be absent if it was not visible on partition images. In the second variation, hypoplasia of one A1 segment of the ACA was defined as a diameter of less than 1 mm on axial partition and maximum intensity projection images. The third variation comprised A1 segments that were slightly asymmetric but were both greater than 1 mm in diameter. In the fourth variation, one posterior communicating artery was larger than the ipsilateral first (or P1) segment of the posterior cerebral artery (hereafter referred to as the *fetal posterior cerebral artery*, or FPCA).

Axial spin-echo images were analyzed for size discrepancies between cavernous ICA flow voids and were cate-

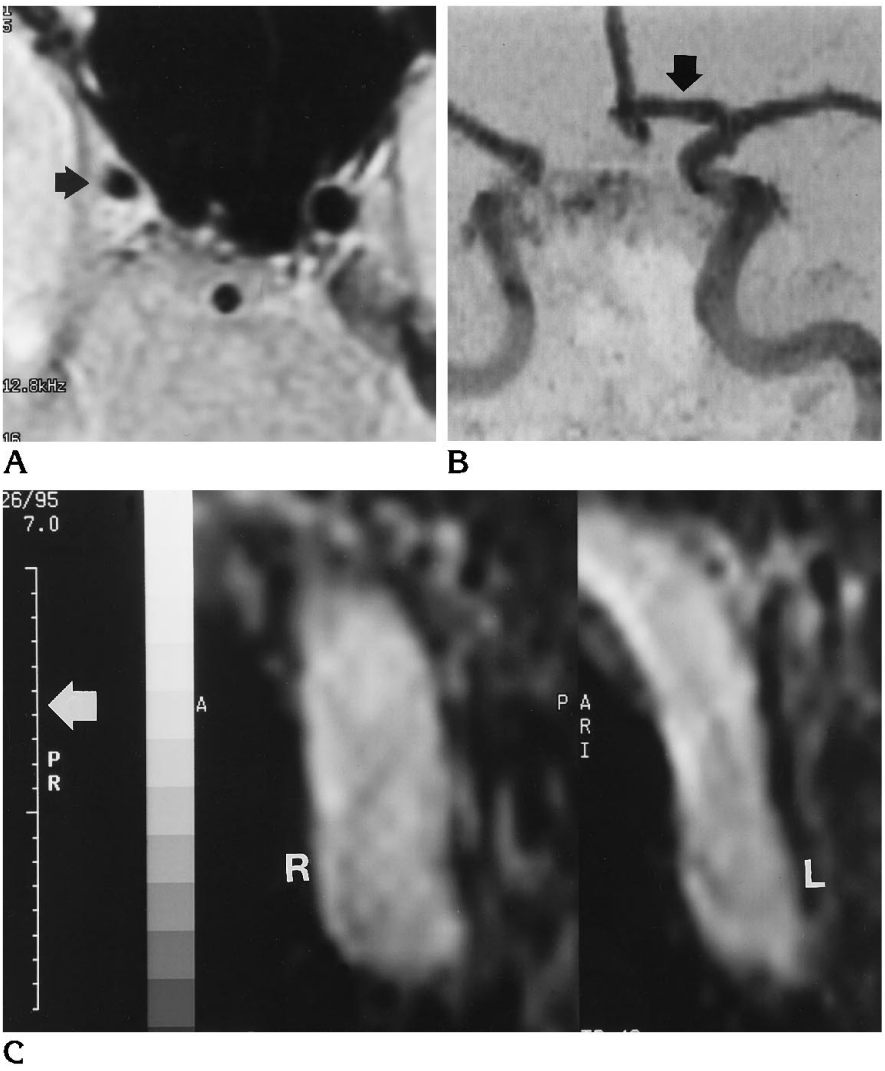

Fig 2. Absent right A1 segment of the ACA.

A, Axial proton density–weighted MR image shows markedly diminished caliber of flow void in right cavernous ICA (*arrow*).

B, Frontal view of maximum intensity projection 3-D time-of-flight MR angiogram shows absence of the right A1 segment with reduced caliber of the ipsilateral ICA. The left A1 segment (*arrow*) is roughly equal in size to the middle cerebral artery.

C, Oblique sagittal multiplanar reformation image through the cavernous carotid arteries reveals a 33% discrepancy in maximum caliber between right (*R*) ICA (4 mm) and left (*L*) ICA (6 mm), as measured at the levels of maximum diameter (original magnification ×7; scale [*arrow*] is in millimeters).

gorized as being equal (no appreciable size discrepancy), slightly asymmetric, or markedly asymmetric.

On the 3-D time-of-flight multiplanar reformation images, we used calipers to measure the maximum axial diameter of the cavernous ICA to the nearest half millimeter (resolution of the MR angiographic partition images was 0.4 to 0.7 mm). Percentages of the difference between the diameters of the right and left ICA for each patient were obtained by dividing the lesser by the greater ICA diameter. A two-tailed *t* test was performed to compare the percentages of difference in diameters among the above categories of normal variations in the circle of Willis. Measurements made on the multiplanar reformation images through the cavernous ICA were repeated to check for intraobserver and interobserver variability.

Results

Results are summarized in the Table. Ten patients had an absent A1 segment (Figs 1 and 2); 10 patients had hypoplasia of one A1 segment (Fig 3); 28 patients had mild discrepancy in the size of the A1 ACA segment; 47 patients had balanced (or equally sized) A1 segments (Fig 4), including four patients with bilateral FPCAs; and nine patients had an isolated unilateral FPCA. Although several other patients had this common variation, they were grouped according to the additional variation present. These are noted in the Table.

The most marked discrepancy in carotid diameters was in the absent A1 category, in which percentages of the difference between diameters ranged from 27% to 40% (mean, 31%). This varied significantly ($P < .00001$) from that noted in the remaining 94 patients. Similarly, the 10 patients with a hypoplastic A1 segment had a mean discrepancy in ICA diameters of

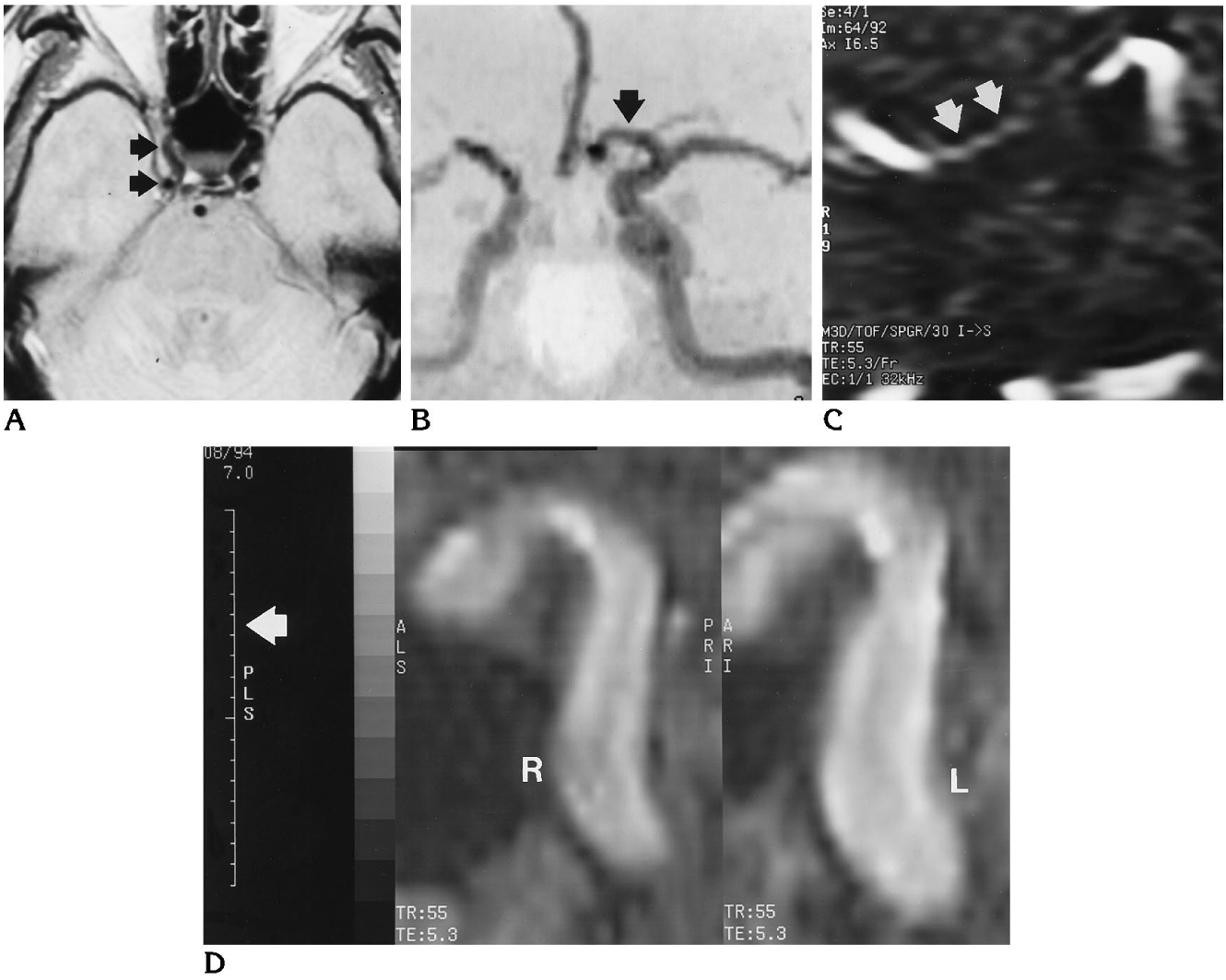

Fig 3. Hypoplastic A1 segment of the ACA.

A, Axial proton density–weighted MR image reveals marked discrepancy in caliber between right and left cavernous ICA, with the right ICA (*arrows*) reduced in caliber.

Frontal view of maximum intensity projection 3-D time-of-flight MR angiogram (*B*) shows enlarged left A1 segment (*arrow*) and does not show hypoplastic right A1 segment, which was 0.4 mm in diameter on the partition image (*arrows* in *C*). Findings on MR angiogram of the neck (not shown) were normal.

D, Oblique sagittal multiplanar reformation image through the cavernous carotid arteries reveals a 20% difference in maximum caliber between right (*R*) ICA (4 mm) and left (*L*) ICA (5 mm), again, as measured at level of maximum diameter (original magnification ×7; scale [*arrow*] is in millimeters).

21%, which varied significantly ($P < .0001$) from the rest of the population. In all 20 of these patients, proximal internal carotid disease was excluded by means of MR angiography of the neck (11 patients), catheter angiography (three patients with absent A1), Doppler sonography (three patients), age less than 40 years (two patients, a 15-year-old girl with tinnitis and a 37-year-old woman with chronic headaches), or history (69-year-old man with isolated high-frequency hearing loss).

Mean discrepancy in ICA diameters in the patients with slightly asymmetric A1 segments ($P > .14$) or a unilateral FPCA ($P > .24$) did not vary significantly from discrepancies noted in the 47 patients with balanced circulation in the circle of Willis.

On axial spin-echo MR images, markedly dis-

Fig 4. Balanced circle of Willis.

Axial proton density–weighted and T2-weighted MR images (*A*) reveal normal symmetric ICA flow voids in patient with symmetric A1 segments shown in *B*, which is a collapsed maximum intensity projection 3-D time-of-flight MR angiogram.

crepant flow voids in the cavernous ICA were noted only in patients with an absent (nine of 10) or hypoplastic (seven of 10) A1 segment. One patient with an absent A1 segment and three of 10 with hypoplastic A1 segments had mildly reduced ipsilateral ICA flow void on axial spin-echo MR images.

Of the remaining 84 patients, 62 had equal-appearing ICA flow void, including three with greater than 50% unilateral proximal ICA stenosis, and 22 had mildly asymmetric carotid flow voids on axial spin-echo MR images. The 22 patients with mildly discrepant ICA flow voids included 13 of 28 patients with differently sized A1 segments, three of nine patients with an isolated FPCA, and six patients with a balanced circle of Willis (equal A1 segments and posterior communicating artery).

Measurements of the diameter of the ICA obtained from the oblique sagittal multiplanar reformation images were identical among observers in 138 of 208 cases, whereas the remaining 70 ICA measurements varied by 0.5 mm in all but one, which varied by 1 mm. None of these interobserver variations produced diameter discrepancies outside the ranges listed in the Table. Similarly, intraobserver ICA measurements were identical on 149 of 208 multiplanar reformation images, with the remaining 59 measurements varying by 0.5 mm.

Discussion

A variety of pathologic conditions may cause unilateral narrowing of the ICA (1–3). This study has shown that asymmetry of the left and right carotid arteries may also result from unilateral absence or hypoplasia of the A1 segment of the ACA, both of which are normal variations in cerebral arterial circulation. Absence of the A1 segment is unusual, occurring in approximately 2% of the population, whereas hypoplasia of one A1 segment occurs more frequently, in up to 10% of the population (4). The cavernous ICA measurements obtained from the oblique sagittal reformations (Figs 3–5) were reproducible to within 0.5 mm in virtually all cases, with interobserver and intraobserver variations explained by ambiguous vessel edges caused by volume averaging of pixels in some cases.

Many pathologic conditions affecting the luminal diameter of the ICA result in focal narrowing, including atherosclerosis, adjacent neoplasm, arteritis, neurofibromatosis, fibromuscular dysplasia, spasm due to adjacent subarachnoid hemorrhage, increased intracranial pressure, meningitis, and radiation therapy (5–7). A more uniform narrowing, such as that seen in our study, might lead one to suspect intimal dissection, particularly in the setting of trauma or acute onset of headache (Fig 5). Prior studies have shown that such a uniform narrowing can result from proxi-

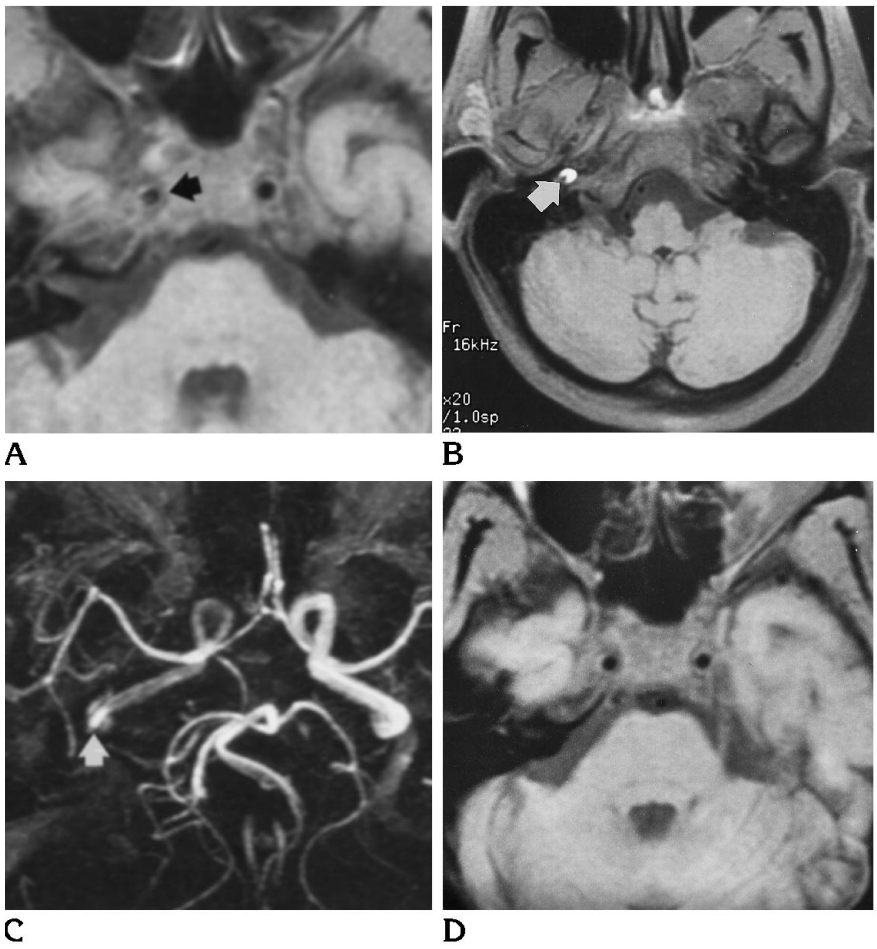

Fig 5. Right ICA dissection in 49-year-old woman with Horner syndrome and right retroorbital headache.

A, T1-weighted fat-saturation axial spin-echo MR image through cavernous segment reveals reduced flow void in right ICA (*arrow*). The rest of the brain MR findings were normal.

B, T1-weighted fat-saturation axial MR image reveals distal right ICA crescent of hyperintensity (*arrow*) from intimal dissection with thrombus and 90% stenosis of luminal diameter.

C, Collapsed 3-D time-of-flight MR angiogram confirms decreased caliber of right petrous and cavernous ICA. Notice the "shine-through" produced by the thrombus in the distal right cervical ICA dissection (*arrow*).

D, Six months later, intracranial axial spin-echo MR image (and MR angiogram, not shown) shows that right cavernous ICA has regained a caliber equal to that of the left ICA after resolution of dissection.

mal stenosis or dissection, but that severe proximal stenosis can also be present in cases in which there is a relatively symmetric appearance to the cavernous carotid arteries on MR images (8). In the case of proximal stenosis (Fig 5), one would also expect diminished flow-related enhancement in the distal ICA and possibly in the ipsilateral middle and proximal ACAs as well, findings that were not present in patients with absence or hypoplasia of the A1 segment. The effect of increased flow from arteriovenous shunting can also result in asymmetry caused by uniform enlargement of the affected side (9).

Although only the cases of absent or hypoplastic A1 were significantly correlated with cavernous ICA asymmetry, the patients with dominant A1 segments and an isolated FPCA tended to have an enlarged ipsilateral cavernous ICA, as seen on both axial spin-echo and MR images and oblique sagittal MR angiographic reformations. Similarly, among patients with an absent A1 segment, the least discrepancy in the ICA diameters (27%) occurred in the patient with an ipsilateral FPCA. In addition, the greatest discrepancy (27%) in ICA diameters among the 10 patients with hypoplastic A1 occurred in two with a contralateral FPCA. There was also a tendency toward larger mean ICA diameters in carotid arteries that gave rise to the FPCA (see Table).

Normally, the greater the area of brain supplied by a vessel, the larger the vessel's diameter; for example, the anterior cerebral artery supplies a major portion of the frontal lobe (10). Temporary occlusion of the anterior cerebral artery results in markedly increased metabolic activity in the parietal and occipital lobes (11). Quantitative flow analysis in the anterior and posterior cerebral arteries may potentially explain why relative enlargement of the cavernous carotid artery occurs on the side supplying both anterior cerebral arteries significantly more often than it does in a carotid artery that gives rise to the posterior cerebral artery. However, in distinction to the FPCA's increasing the size of the ipsilateral ICA, absence or hypoplasia of one A1

segment most likely increases the size of the contralateral ICA as well as decreases demand on the ipsilateral ICA.

The diameter range for the preophthalmic ICA within 1 standard deviation in our series (3.8 to 5.3 mm) correlates well with previous autopsy data (3.3 to 5.4 mm) (12). Although one prior autopsy report identified a connection between discrepancies in the size of the supraclinoid carotid artery and hypoplasia of the A1 segment, the observation is not commonly made during catheter angiography, perhaps because of variable magnification with each single-vessel injection (13). Hypoplasia of one A1 segment has been associated with an increased frequency of aneurysms of the ACA (14).

Care must be taken when interpreting MR images of the brain to ascertain patency of major arterial and venous structures. Our study has shown that significant asymmetry in the size of the carotid arteries occurs when one A1 segment is hypoplastic or absent. While carotid asymmetry should always be viewed with suspicion, the important association outlined in this study, and detectable on MR angiograms, may be useful in resolving discrepancies when the index of clinical suspicion of more serious disease is low.

References

1. Hilal SK, Soloman GE, Gold AP, et al. Primary cerebral artery occlusive disease in children, I: acute acquired hemiplegia. *Radiology* 1971;99:71–86
2. Sekhar LN, Dujovny M, Rao GR. Carotid-cavernous sinus thrombosis caused by *Aspergillus fumigatus*. *J Neurosurg* 1980;52: 120–125
3. Wollschlaeger G, Wollschlaeger PB, Lopez VF, et al. A rare cause of occlusion of the internal carotid artery. *Neuroradiology* 1970; 1:32–38
4. Mitchell DG, Merton DA, Mirsky PJ, Needleman L. Circle of Willis in newborns. *Radiology* 1989;172:201–205
5. Brant-Zawadzki M, Anderson M, Dearmond SJ, et al. Radiation-induced large-vessel occlusive vasculopathy. *AJR Am J Roentgenol* 1980;134:51–55
6. Toboada D, Alonso A, Moreno J, et al. Occlusion of the cerebral arteries in Recklinghausen's disease. *Neuroradiology* 1979;18: 281–284
7. Hilal SK, Solomon GE, Gold AP, et al. Primary cerebral arterial occlusive disease in children, II: neurocutaneous syndromes. *Radiology* 1971;110:87–93
8. Brant-Zawadzki M. Routine MR imaging of the internal carotid artery siphon: angiographic correlation with cervical carotid lesions. *AJR Am J Roentgenol* 1990;155:359–363
9. Newton TH, Troost BT. Arteriovenous malformations and fistulae. In: Newton TH, Potts DG, eds. *Radiology of the Skull and Brain*. St Louis: CV Mosby; 1974:2494
10. Montemurro DG, Bruni JE. *The Human Brain in Dissection*. Philadelphia, Pa: WB Saunders; 1981:32
11. Medina M, Melcarne A, Musso C, et al. Variations in regional cerebral blood flow investigated by single photon emission computed tomography with technetium-99m-d, 1-hexamethylpropyleneamineoxime = 1-h during temporary clipping in intracranial aneurysm surgery. *Neurosurgery* 1993;33:441–449
12. Hayreh SS. Arteries of the orbit in the human being. *Br J Surg* 1963;50:938–953
13. Baptista AG. Studies on the arteries of the brain, III: circle of Willis, morphologic features. *Acta Neurol Scand* 1964;40:398–414
14. Kayembe KN, Sasahara M, Hazama F. Cerebral aneurysms and variations in the circle of Willis. *Stroke* 1984;15:846–850